Breakup simulation of a viscous liquid using a coaxial high-speed gas jet

Q. Ye*[1], B. Shen[2], O. Tiedje[1]
[1]Fraunhofer Institute for Manufacturing Engineering and Automation, Stuttgart, Germany
[2]University of Applied Sciences, Esslingen, Germany
*Corresponding author: Qiaoyan.ye@ipa.fraunhofer.de

Abstract
This paper presents numerical simulations of the atomization of viscous liquids, focusing on the combination of the liquid breakup and droplet transport processes. Coaxial high-speed gas jet created by a High Volume Low Pressure (HVLP) spray gun was used. The VOF-to-DPM model, namely coupled Volume of Fluid and Lagrangian particle tracking approaches, was applied. Secondary breakup model was also applied. Effect of breakup models and grid size on the droplet distribution was studied. The intact liquid length close to the liquid nozzle and the formation of liquid droplets in the regions of primary and fully developed breakup along the spray jet and the spray angle directions were analysed. The Sauter mean diameter distribution and the droplet-velocity correlation downstream the nozzle were compared with experimental results.

Keywords
Viscous liquid breakup, coaxial high-speed gas jet, coupled VOF and Lagrangian particle tracking approaches.

Introduction
Coaxial high-speed gas jets are widely used to atomize paint liquids in industrial painting processes, such as using pneumatic or HVLP (High Volume Low Pressure) spray guns, where the liquid jet is broken up in a high-speed annular gas stream. Usually, a critical state with sonic speed does exist around the exit of the liquid jet. At the same time, a so-called shaping gas flow is used to form the spray pattern. Some experimental and numerical studies [1-3] of air and air-assisted spray guns have been carried out in the past, focusing mainly on the characterization of droplet size distribution, on the effects of air flow and on the particle trajectory. Conventionally, in order to perform spray painting simulation, namely the prediction of the droplet transport and the resulting film thickness distribution on a workpiece, empirical assumptions for the initial conditions of the droplet phase at the droplet inlet plane are required, i.e., positions, velocity vectors and concentrations. Furthermore, droplet size distributions measured at locations further downstream, where droplet formation is fully developed, had to be applied.

Although some research work has been done to investigate the primary breakup of coaxial liquid-gas jets [4-9], few of those investigations focused on the atomization by a sonic-speed gas jet. In our previous study [10], the initial breakup of a paint liquid in a HVLP spray gun with high-speed gas jet was investigated numerically. The Volume of Fluid method (VOF) was applied. Images of jet instabilities and primary atomization in the region close to the nozzle were used to analyse the intact liquid length and the effect of the shaping gas jet on the atomization process, in order to elucidate the dominant mechanisms in the primary breakup of the liquid jet. The prediction of full breakup processes in such an atomizer is nowadays still an open research topic, since the simulation of a complete spray process using VOF method requires very fine local grids, which makes it unrealistic for practical applications.

Concerning the numerical simulation of primary atomization of a liquid jet, there are many research work, such as large eddy simulation for turbulent liquid/gas phase interface dynamics [11], using VOF and direct numerical simulation (DNS) to investigate the instabilities on liquid sheets [12], primary breakup of a diesel jet using high resolution DNS with lever set method [13] and an investigation of primary breakup of shear-thinning jets exit using DNS [14]. A full spray simulation of a liquid jet was carried out [15] using coupled VOF and Lagrangian particle tracking methods, in order to reduce the computational cost.

Only very few breakup simulations exit for liquid jets with a coaxial high-speed gas jet. The purpose of the present study is to carry out numerical simulation of the atomization of viscous liquids, focusing on the combination of the liquid breakup and droplet transport processes. The numerical simulations were carried out using the commercial CFD code ANSYS Fluent. The VOF-to-DPM model, namely coupled Volume of Fluid and Lagrangian particle tracking approaches, was used. Secondary breakup model was also applied. Effect of secondary breakup models and grid size on the droplet distribution was studied. The intact liquid length close to the liquid nozzle and the

formation of the liquid droplets in the regions of primary and fully developed breakup were analysed. Droplet size distributions downstream the nozzle were compared with experimental results.

Numerical methods

The basic geometry of a HVLP-spray gun used in this study is shown in Figure 1. Atomization occurs by a coaxial jet arrangement, in which the central paint jet with the diameter of 1.3 mm is surrounded by high-speed air, leaving the annular ring around the paint nozzle under sonic conditions. Around the annular ring, there are four small holes with 0.6 mm diameter, from which the high-speed air is supplied. In addition, the so-called shaping air nozzles with 2 mm diameter on the two sides of the centre jet are used to deform the spray cone for painting larger work pieces.

The commercial CFD code ANSYS Fluent, based on the finite-volume approach, was used for the numerical simulations. A polygonal mesh with 7 million cells was used to discretize the computational domain of 300×300×110 mm³, as shown in Fig.2. Mesh refinement with cell resolution $\Delta x \approx 30\mu m$ close to the liquid nozzle was made. On the boundaries of the computational domain, inlet profiles near the atomizer for airflow quantities, such as velocity components and turbulence parameter, were used based on the simulation results obtained from the numerical study [16] using large computational domain. Far away from the atomizer ambient pressure was used. Atomizer operating conditions and the liquid properties are shown in Table 1. The clear paint shows a weak shear-thinning non-Newtonian behaviour. A constant viscosity of 40 mPa·s obtained according to the strain rate quite close to the atomization airflow nozzle was applied.

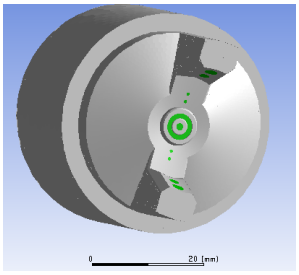

Table 1. Atomizer characteristics and liquid properties

Atomizing air flow rate	0.0037 kg/s
Shaping air flow rate	0.0045 kg/s
Liquid flow rate	150 g/min
Liquid phase	Clear paint
Liquid density and surface tension	1000 kg/m³, 0.03 N/m
Liquid viscosity	40 mPa·s

Figure 1. a HVLP spray gun atomizer

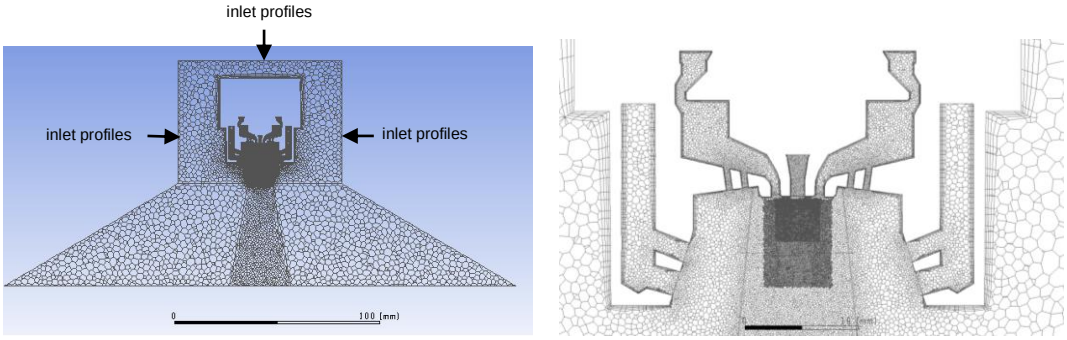

Figure 2. Computational domain and mesh model

The gas phase was modelled using the Eulerian conservation equations of mass, momentum, and energy. The 3D compressible airflow was simulated. As inlet boundary conditions, air mass flow rate and stagnation temperature were used at the air nozzles. Turbulent transport was modelled using the Realizable k-ε model with scalable standard wall function. After getting convergent solution of the airflow field, time-dependent VOF-to-DPM (Volume of Fluid – Discrete Phase Model) simulations for the liquid jet breakup were performed using the coupled VOF and Lagrangian particle tracking approach. The VOF-to-DPM model can reduce the computational expense of a VOF breakup simulation due to its ability to transfer VOF-lumps to DPM droplets. For the VOF-lump conversion requirement we used the asphericity parameter of 0.3, which means that a VOF-lump will transfer to a DPM-parcel if asphericity is below this criterion. Gradient adaption on the VOF-interface was applied in the dynamic mesh model, which allows dynamic local refinement or coarsen of the mesh. It was found that solution divergence occurs very often by continuously increasing mesh refinement level, especially for the current compressible airflow field coupled with two phase flow. Therefore, mesh size of about 20 – 30 µm close to the

liquid nozzle was kept for the primary jet breakup. Secondary droplet breakup models, such as the wave model [17] and the stochastic secondary droplet (SSD) model [18] were then added to calculate the further droplet breakup. In the wave model droplet breakup is determined using a single diameter scale, while the SSD model treats particle-breakup as a discrete random process resulting in a distribution of diameter scale over a range. Default parameters in breakup models, such as the droplet critical We_{cr} number in the SSD model, are applied in the present simulation. With We_{cr} the critical droplet radius based on the local cell conditions can be calculated. Drops larger than this critical radius are subject to breakup. Effect of breakup models on the size distributions was then analysed at the downstream spray jet. Droplet coalescence model is not considered in this study. A typical time steps of 0.01 – 0.1 µs in the simulations has to be used. Simulations were mainly carried out with reasonable parallel processors of 240 using Cray XC40 (Hazelhen) at High Performance Computing Centre Stuttgart.

Results and discussion

At first, air flow using k-ε turbulence model was carried out without liquid phase. On the boundaries of the computational domain room-temperature and ambient pressure were applied. Figure 3 shows the air velocity close to the atomizer. High velocities about 360 m/s can be observed at the air nozzles. Direct under the liquid nozzle and quite close to the atomizing airflow ring there are large eddies, as shown in Fig. 3b, where the velocity vectors are depicted in the range of 10-120 m/s. The flat spray jet, as shown in Fig. 3c, is created because of the shaping air flow jets. A quite narrow peanut-shape flow region (Fig. 3d) is formed downstream the nozzle.

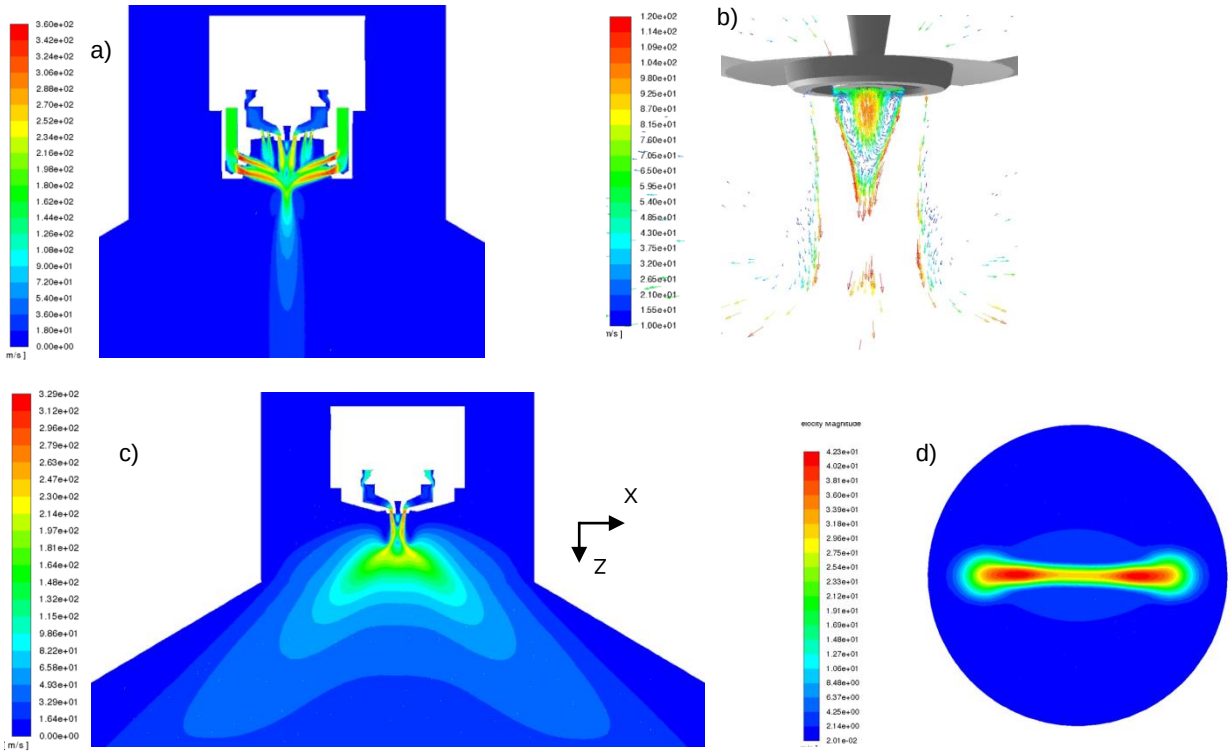

Figure 3. Air velocity field (m/s), a): in the cross-section x = 0, b): Velocity vectors near the liquid nozzle; c): in the cross-section y = 0, d) in the cross-section z = 50mm.

VOF-to-DPM simulations were then carried out. Liquid is injected with room-temperature into the domain. The Liquid velocity on the nozzle exit is about 2 m/s, whereas air velocity around the liquid can be 50 - 250 m/s. The large relative gas-liquid velocity and the high strain-rate of the mixture (ca. 5e5 1/s) in the interface result in quick breakup of liquid film/ligament. The non-dimensional parameters Re_l and We based on the liquid nozzle diameter are defined as:

$$Re_l = \frac{\rho_l U_l D_l}{\mu_l}, \quad We = \frac{\rho_g (U_g - U_l)^2 D_l}{\sigma}$$

where ρ_l and ρ_g are the liquid and gas densities, respectively, U_l and U_g liquid and gas velocities, μ_l the liquid dynamic viscosity, and σ the surface tension. In the present case the Re_l and We are 65 and 3200, respectively. A snapshot of liquid-gas boundary with a value of the liquid volume fraction of 0.5 is shown in Fig.4a. Figure 4b shows the overlay of velocity contours (0 – 200 m/s) with VOF-liquid (magenta colour). Liquid ligaments and lumps can be observed. It was found that the intact liquid length, the main core length, is less than 5 mm, far away from the cross point of the shaping air jets at about 9 mm downstream the liquid nozzle. Raynal [19] and Shen *et. al.* [10] predicted intact liquid length of an atomizer with coaxial high-speed gas jet using correlations

$L/D_l \approx 6/M^{0.5}$ and $L/D_l \approx 10.04/M^{0.552}$, respectively, where M is dynamic pressure ratio $M = \rho_g {U_g}^2/\rho_l {U_l}^2$ and D_l is diameter of liquid nozzle. The intact liquid length in Fig. 4 is about 2.5 mm, quite close to the proposed equation in [10].

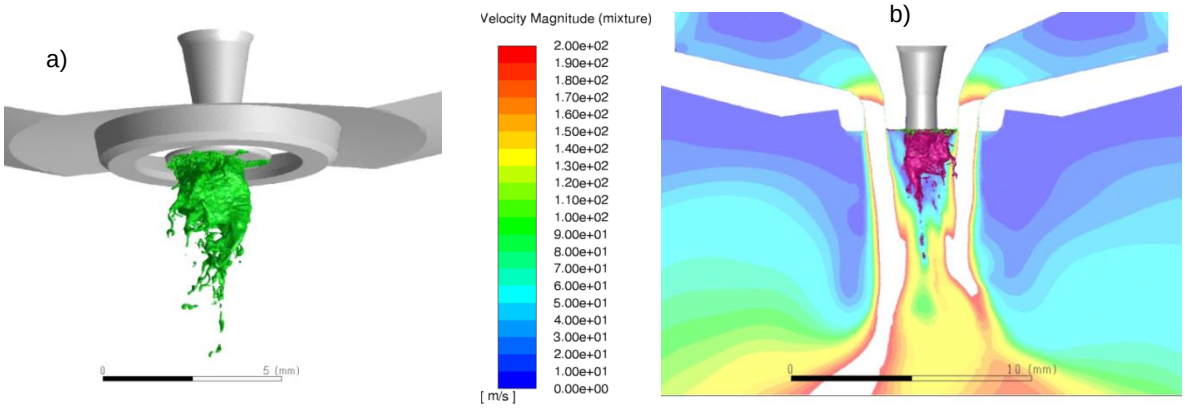

Figure 4. a): a): Detailed view of VOF-liquid (volume of fraction = 0.5); b): Velocity contours (0 - 200 m/s) overlaid with VOF-liquid (Volume of fraction = 0.5, magenta colour).

Transfer of liquid VOF-lumps to DPM-droplets occurs if some criteria are met, such as the asphericity limit of 0.3 is used in the present study. The corresponding spray evolution is depicted in Fig.5. The resulting droplet size is clearly too large, which is far away from experimental observations. For the present study, it is not realistic, to carried out atomization simulations with further mesh refinement and much smaller time step. Therefore, based on the created primary droplets, breakup models were applied. Figure 6 and 7 show snapshots of a spray jet using the Wave model and the stochastic model (SSD), respectively. Large droplets can be observed close to the liquid nozzle in both cases. Droplets undergo breakup mainly in the region z < 10mm. Basically, SSD-model produces much more small size droplets than wave-model. In order to show the spray evolution quantitatively, Sauter mean diameters (D_{32}) were evaluated along the spray jet direction and compared with experimental results [11] that were obtained at z = 50 mm using Malvern Spraytec Fraunhofer type particle sizer. As shown in Fig. 8, D_{32} is about 92 µm without breakup model and 27 µm with the Wave model. The Sauter mean diameter D_{32} = 8 µm obtained from the SSD-model is quite close to the experimental result (7 µm).

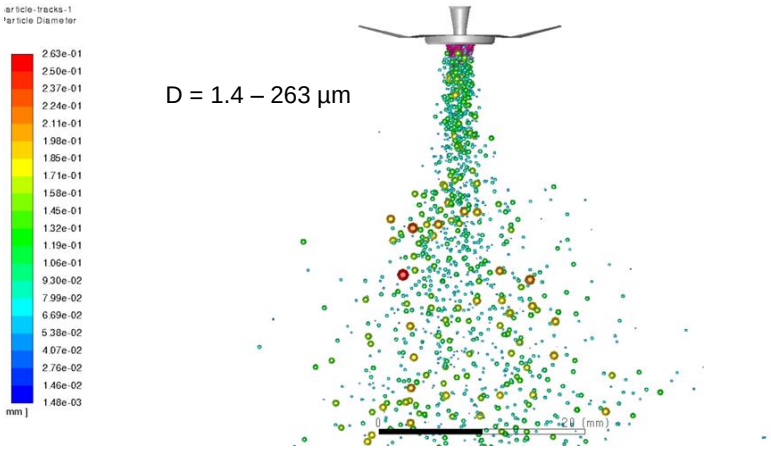

Figure 5. Instantaneous snapshot of spray evolution without breakup model, image size scale of the sphere is 5.

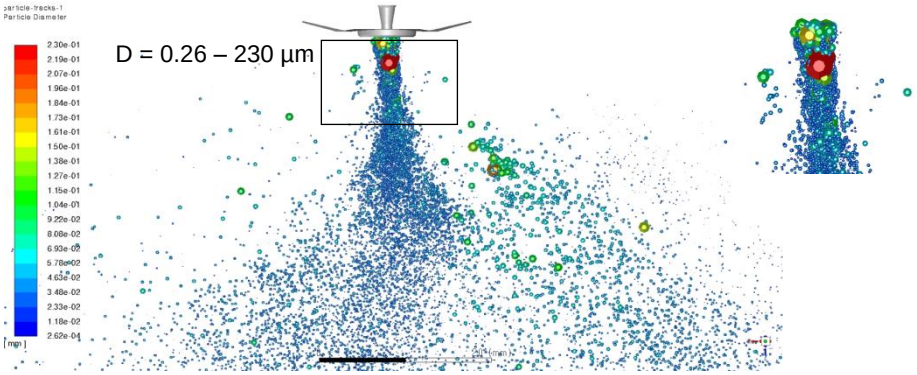

Figure 6. Instantaneous snapshot of spray evolution using the wave-model for secondary breakup, image size scale of the sphere is 10.

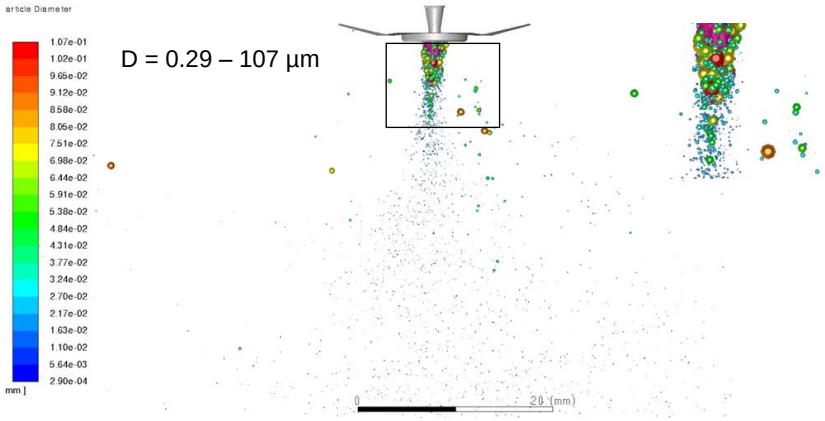

Figure 7. Instantaneous snapshot of spray evolution using the SSD breakup model, image size scale of the sphere is 10.

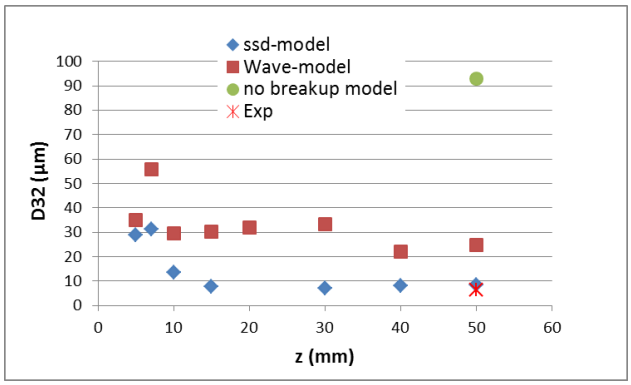

Figure 8. Sauter mean diameter distribution along z-direction (spray jet direction).

By quasi-developed spray jet, i.e. after approx. 2 ms, the number of computational particles in the domain is stable for a given time step, namely about 27000 for the SSD model and 30000 for the Wave-model. More detailed analysis of droplet distributions was then performed based on the simulation results with the SSD-model. Figure 9 (a) shows the Sauter mean diameter distribution along the flat-spray angle direction. A very good agreement with experimental results was obtained. Far away from the jet centre droplet size is decreased. However, a few quite large droplets are located at the spray jet edges, which can be understand by observing the spray image in Fig. 7. Generally, at the spray edges droplet concentration is low and the results are quite sensitive to the data rate for both simulation and experiment. Nevertheless, the similar trend at the spray edges for both the simulation and the experiment can be observed. The droplet concentration at the cross-section of z =

50 mm is depicted in Fig. 9 (b). The small concentration region (0 - 1e-4 kg/m³) is used, in order to get the image contour clearly. This image contour is quite similar to the velocity contours in Fig.3 (d), since small droplets can follow the air flow.

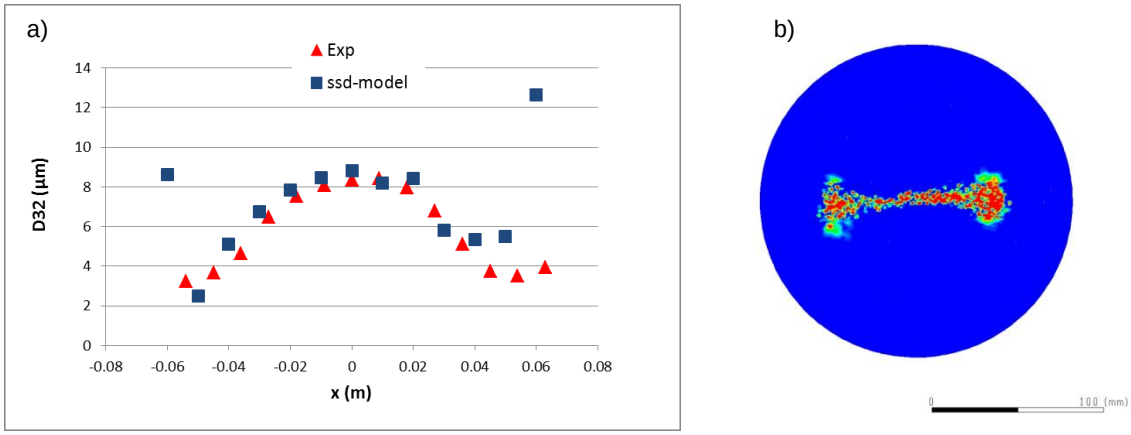

Figure 9. a) Sauter mean diameter distribution at z = 50 mm along x-direction (flat-spray angle); b) Particle concentration distribution at the cross-section z = 50mm, red colour: particle concentration > 1e-4 kg/m³.

Total particle distributions are further analysed by sampling all particles at two cross-sections, namely z = 5 mm near the liquid nozzle and z = 50 mm. For simplicity, ΔD = 1µm was used for grouping of particles. Figure 10 shows the size distributions at z = 5 mm, at which the maximum particle size is about 240 µm. In Fig. 10 only droplets in the range from 1 – 100 µm are depicted. Although there are some large droplets in this cross-section, the mass fractions of droplets large than 50 µm are low and quite scattered. The velocity-droplet correlation (Fig. 11) shows high velocity for small droplets, such as 160 m/s for 1 µm particle, since the created small particles can quickly follow the air flow, whereas the initial velocity of large droplets are relative low. The mass fraction of small drops (< 2 µm) in this cross-section is relative high. So far, it is not clear if these quite small droplets result from numerical diffusion of the VOF-Simulation. However, it should be noted, that measurements performed further downstream at larger distances to the bell confirm the presence of this small size fraction. In any case, this group of droplets has no significant effect for the spray painting applications, since their mass fraction is still quite low.

At the cross-section z = 50mm large droplets were not found, as shown in Fig. 12. The maximum particle is about 25 µm. A few large particles, as shown in Fig. 7, escaped from the current cone-shaped computational domain boundaries (Fig. 2). Comparing to the Fig. 11, the velocities of small particles are about 40 m/s, as shown in Fig. 13, since the drag force makes the small droplets slowdown. During the spray evolution many large particles are accelerated in the region z < 10 mm and reach the cross-section z = 50 mm with higher velocity because of the inertia force. This trend of velocity-droplet correlation at z = 50 mm can be validated (Fig.13 (b)) using experimental results obtained with Phase-Doppler Anemometer (PDA), in which a similar spray gun and atomization air flow rate were used. The used liquid flow rate was 250 g /min in the experiment, higher than in Fig. 13 (a), therefore there are more large droplets in Fig. 13 (b). Moreover, the measurement result corresponds to a local value, namely in the spray jet centre. However, the trend of Figure 13 (a) and (b) is considered to be reasonable.

It should be noticed that in particle size measurements relative enough data rate at each measuring point was applied, such as 20 000 samples by PDA and a few seconds sampling time by Spraytec Fraunhofer type particle sizer, which ensures to catch a certain number of large size particles. Although the simulated Sauter mean diameters using the SSD breakup model are quite close to the experimental results, lack of large particles or narrow particle size spectrum in the present simulation is clearly. The sampling time in the present simulation is only 2-3 ms that is actually not enough for catching large size particles. In the present study droplet coalescence was neglected, which is probably another reason that we obtained less large particles. The default parameters in breakup models were applied in the present study. Effect of parameters in breakup models on the size spectrum, such as in SSD-model, should be investigated.

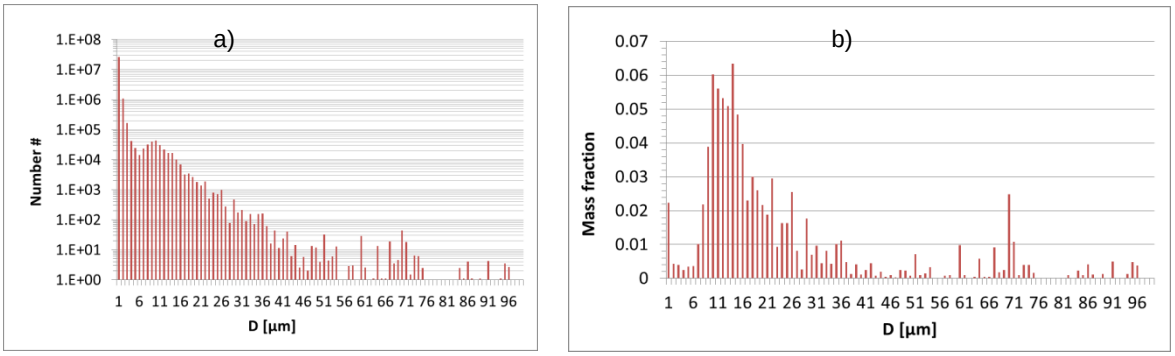

Figure 10. Droplet size distributions at z = 5 mm. a) Number distribution, b) Mass fraction distribution.

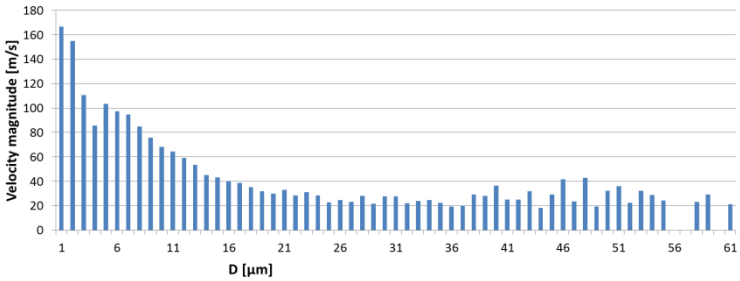

Figure 11. Droplet size and velocity correlation at z = 5 mm

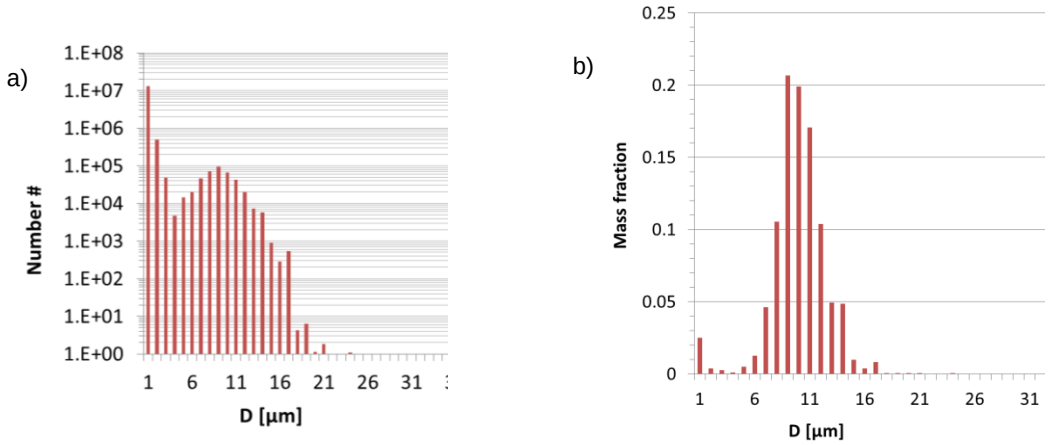

Figure 12. Droplet size distributions at z = 50 mm. a) Number distribution, b) Mass fraction distribution.

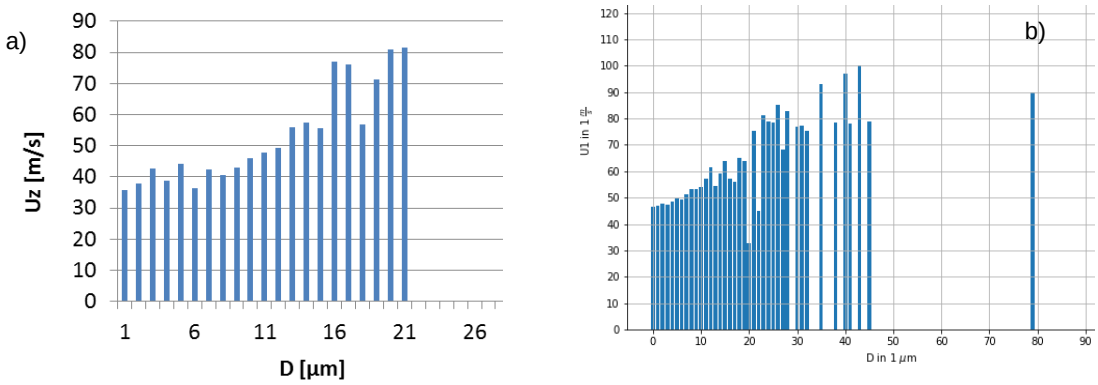

Figure 13. Droplet size and velocity correlation at z = 50 mm (axial velocity vs. droplet diameter). a) Simulation results, b) Experimental results using PDA

Conclusions

Numerical study of atomization of viscous liquids using a coaxial high-speed gas jet, focusing on the combination of the liquid breakup and droplet transport processes, were carried out. Coupled Volume of Fluid and Lagrangian particle tracking approaches were applied. Instead of using extremely fine mesh, secondary breakup model based on the parent droplets created by VOF-to-DPM method had to be used, to keep away from convergent difficulties in the present simulation for the complicated two phase flow near the liquid nozzle.

Spray jet evolution was analysed in the jet and the flat-spray angle directions. It was found that the intact liquid length is smaller than 5 mm for the present operating conditions. In this region transfer of VOF-lumps to initial droplets occurs and large size droplets can be observed, corresponding to the primary breakup event. Droplets undergo further breakup mainly in the region z < 10mm. Effect of secondary breakup models on the droplet size distributions was studied. The results of breakup simulation were validated against available experimental data in downstream spray jet, namely at z = 50 mm. The Sauter mean diameter distribution and the droplet size-velocity correlation obtained using the SSD breakup model agree very well with the experiment. However, it is missing large size droplets using the SSD model for the present application. Further breakup simulation should be carried out with the consideration of droplet coalescence model. Data rate for the analysis of particle size distribution should be increased and effect of parameters in secondary breakup models on the size distribution for the current application should be further investigated.

Acknowledgements

The present work has been supported by the High Performance Calculation Centre Stuttgart (German federal project: PbusRobe). This support is gratefully acknowledged by the authors.

References

[1] Domnick, J.; Lindenthal, A.; Tropea, C.; Xu, T.-H. Application of Phase-Doppler anemometry in paint sprays. Atomization and Sprays **1994**, 4, 437–450.
[2] Ye, Q., Shen, B., Tiedje, O., Bauerhansel, T., Domnick, J., 2015, Atomization and Sprays, 25 (8), pp. 643-656.
[3] Ye,Q. and Pulli, K., 2017, Coatings, 7,13.
[4] Lasheras, J. C., Hopfinger, E. J., *Annual Review of Fluid Mechanics* 32: 275-308 (2000)
[5] Varga, C. M., Lasheras, J. C., Hopfinger, E. J., *Journal of Fluid Mechanics* 497: 405-434 (2003)
[6] Funada, T., Joseph, D. D., Yamashita, S., *International Journal of Multiphase Flow* 30: 1263-1310 (2004)
[7] Matas, J. P., Marty, S., Cartellier, A., *Physics of Fluids* 23: 094112 (2011)
[8] Gautam, V., *Flow and atomization characteristics of cryogenic fluid from a coaxial rocket injector*, PhD thesis, University of Maryland, 2007
[9] Matas, J. P., Cartellier, A., *Comptes Rendus Mécanique* 341: 35-43 (2013)
[10] Shen, B., Ye, Q., Tiedje, O., Westkämper, W., Aug. 23-27. 2015, 13th Triennial International Conference on Liquid Atomization and Spray Systems.
[11] Herrmann, M., Aug. 23-27, 2015, 13th Triennial International Conference on Liquid Atomization and Spray Systems.
[12] Sander, W. and Weigand, B., Phys. Fluids, vol.20, no.5, p. 053301 (2008)
[13] Shinjo, J. and Umemura, A., *Intenational Journal of Multiphase flow, 37. 1294-1304 (2011)*
[14] Ertl, M. and Weigand, B., Atomization and Sprays 2017, 27, 303 – 317.
[15] Grosshans, H., Szász, R-Z.,Fuchs, L., Sept. 2011, 24th European Conference on Liquid Atomization and Spray Systems, Estoril, Portugal.
[16] Ye, Q., Tiedje, O., Srinivas, S.R., Noest, T., Uhrner, U., Sept. 6-8. 2017, 28th European Conference on Liquid Atomization and Spray Systems.
[17] Reitz, R.D., Modeling atomization processes in high pressure vaporizing sprays, 1987, Atomization Spray Tech. 3,307.
[18] Apte, S.V., Gorokhovski, M.,Moin, P., Intenational Journal of Multiphase flow, 29. 1503-1522 (2003)
[19] Raynal, L., Instabilité et entraînement à l'interface d'une couche de mélange liquid-gaz, PhD thesis, Université Joseph Fourier, 1997